1526 *Macromolecules* **2003,** *36,* 1526−1533

Discotic Liquid Crystalline Triblock Copolymers: Interplay of Liquid Crystal Architecture with Microphase Separation

Rukmal Abeysekera,[§] Richard J. Bushby,*,[†] Celine Caillet,[‡] Ian W. Hamley,[‡] Owen R. Lozman,[†] Zhibao Lu,[†] and Anthony W. Robards[§]

The Centre for Self-Organising Molecular System, University of Leeds, Leeds LS2 9JT, UK; School of Chemistry, University of Leeds, Leeds LS2 9JT, UK; and Institute for Applied Biology, Department of Biology, University of York, York YO10 5BQ, UK

Received May 16, 2002; Revised Manuscript Received December 11, 2002

ABSTRACT: A triblock copolymer has been prepared in which a main chain polymeric discotic liquid crystal is capped at both ends with blocks of poly(ethylene oxide). It has been characterized by GPC, DSC, polarizing microscopy, small- and wide-angle X-ray diffraction, electron microscopy, and rheometry. The copolymer undergoes microphase separation, giving a nanostructured material consisting of a hexagonal array of poly(ethylene oxide) rods in a matrix of columnar liquid crystal. It is found that the alignment of these rods is determined by that of the liquid crystal. Hence, under shear, both the columns of the discotic and the rods of poly(ethylene oxide) align perpendicular to the shear direction. At lower temperatures the poly(ethylene oxide) regions crystallize, and a lamellar structure is obtained.

Introduction

Polymers that incorporate mesogenic moieties have considerable application potential in a range of advanced electrooptic and organic semiconductor technologies.[1−3] At the root of this potential is the unique duality of properties exhibited, specifically, the combination of macromolecular characteristics such as mechanical integrity and ease of processability, with the anisotropic properties of low molar mass liquid crystals.[1] Similarly, block copolymers have attracted attention because it is possible to tailor the properties by combining blocks with distinct characteristics (glassy, rubbery, crystalline). In addition, they form a range of microphase-separated structures. For diblock copolymers these are lamellae, hexagonal-packed cylinders, cubic-packed spheres, and a bicontinuous cubic gyroid morphology (depending on temperature and volume fraction).[4] The coupling of a mesogenic block to an isotropic block in a side-group liquid crystal block copolymer leads to a fascinating interplay between liquid crystalline order and the microphase separated order. The mesogen influences the microphase structure of the block copolymer and vice versa.[5] It has been reported that the region of stability of the lamellar phase is enhanced in certain side-group liquid crystal polymers compared to coil−coil diblocks,[6] although not in others,[7] and it may be shifted in composition range.[6,8] The origin of these phase boundary shifts is the change in interfacial curvature, resulting from the elastic properties of the liquid crystalline block. Microphase separation also influences the conformation of the liquid crystalline block and the orientational ordering of the mesogens. The conformation of the liquid crystalline block is constrained by the coupling of this block to the isotropic block.[9] This is similar to the situation in amorphous−crystalline block copolymers, where the folding of the crystalline block is influenced by the amorphous block.[10] Equilibrium chain folding can occur (in contrast to homopolymers) due to the requirement to balance the interfacial area of both blocks. The orientation of the mesogens with respect to the microstructure can be probed on samples aligned by flow.[6,7,11,12] It will depend on the composition of the copolymer (which in turn controls the microphase symmetry) and on the size of the microphase-separated domains (finite size effect).[9] If the liquid crystal is confined within spheres, smectic phase formation is suppressed, and instead a nematic phase has been observed.[7,11] In contrast, when the liquid crystalline domain is continuous, smectic phases can form. Considering, for example, lamellar phases, the smectic layers are usually aligned perpendicular to the block copolymer lamellae.[7,9,12−14] However, a parallel alignment has been reported for a smectic C*-forming mesogen.[15] It was proposed that the distinct orientation resulted from a decoupling of mesogenic order from that of the block copolymer due to the longer spacer attaching the mesogen to the backbone. A homogeneous orientation of mesogens parallel to the walls of cylinders has been reported.[12,16] For the inverse structure (continuous liquid crystalline phase) smectic layers lie parallel to the cylinders[7] or tilted with respect to them.[6] Liquid crystal phase transition temperatures are usually found to be similar to those of the corresponding homopolymers (although the transition enthalpy may differ).[9] However, Zheng and Hammond report a stabilization of the smectic phase by the lamellar block copolymer microstructure.[17] Liquid crystalline phase transitions also influence the microphase structure. For example, the isotropic−nematic transition for one polymer was observed to induce a transition in the microphase-separated morphology (from body-centered-cubic spheres to cylinders).[18] In another case, a transition from a mixed lamellar/cylinder morphology to a pure lamellar morphology was induced by the change in interfacial curvature resulting from the loss of liquid crystalline ordering.[16] Previous work with side chain smectic liquid crystal block copolymers has shown that the smectic layers can lie parallel or perpendicular

---

[†] The Centre for Self-Organising Molecular System, University of Leeds.

[‡] School of Chemistry, University of Leeds.

[§] University of York.

* Corresponding author: e-mail r.j.bushby@chem.leeds.ac.uk.

10.1021/ma020748x CCC: $25.00

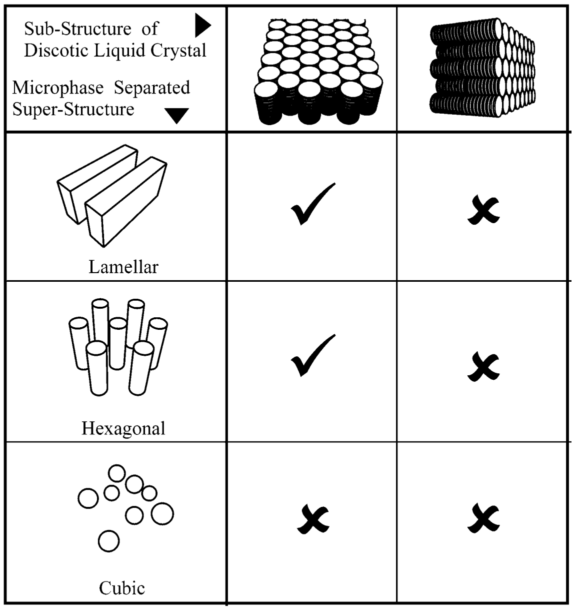

Figure 1. Likely compatibility of the microphase-separated structures of block copolymers with an underlying columnar hexagonal liquid crystal architecture.

to the shear direction, depending on the volume fraction of the mesogen.[19−21] This has been attributed to the difficulty in forming smectic phases with very few layers.

In this paper we begin to address the extent to which this behavior is replicated when the calamitic liquid crystal moieties are replaced with discotic mesogens so that one or both of the phase-separated regions have the substructure of a columnar liquid crystal.[22,23] In the single example described in this paper we show that both phase-separated cylinder and lamellar superstructures are formed. Figure 1 shows that these superstructures are easy to reconcile with a columnar discotic liquid crystal substructure provided they have the relative orientations shown. On the other hand, cubic microphase-separated superstructures seem unlikely, as do the columnar and lamellar superstructures shown on the right-hand side of Figure 1. Hence, there should be a direct correlation between the orientation of the liquid crystal substructure and that of the microphase-separated superstructure, and methods that can be used to align the liquid crystal substructure should also align the phase-separated superstructure. In brief, block copolymers in which one or both of the blocks are a columnar discotic liquid crystal should show simplified phase behavior, and it should be easier to fabricate bulk aligned samples.

The triblock copolymers that we have prepared have a main chain polymeric discotic liquid crystal capped at both ends with blocks of poly(ethylene oxide) (PEO).[23] The triblock copolymer capped with PEO2000 has been characterized by GPC, DSC, polarizing microscopy, small- and wide-angle X-ray diffraction, electron microscopy, and rheometry. It undergoes microphase separation to give both columnar and lamellar structures. Under shear, the columns of the microphase-separated cylindrical phase, like the columns of a main chain discotic polymer columnar mesophase, orient perpendicular to the shear direction.[24−31] This contrasts to the hexagonal phases of most phase-separated block copolymers where the columns orient parallel to the shear direction.[32]

Experimental Section

Synthesis. *2,7-Dihydroxy-3,6,10,11-tetrahexyloxytriphenylene* (**6a**) was synthesized as shown in Figure 2, using published procedures and elaborated into the block copolymer MCBP2000 **10** as shown in Figure 3.[24]

2,7-Bis(2-ethyloxyacetoxy)-3,6,10,11-tetahexyloxytriphenylene (**6b**). A mixture of 2,7-dihydroxy-3,6,10,11-tetrahexyloxytriphenylene (**6a**) (1.32 g, 2 mmo1), ethyl 2-bromoacetate (1 g, excess), and cesium carbonate (1.30 g, 4 mmol) in *N*-methyl-2-pyrrolidinone (NMP, 10 mL) was heated at 110 °C for 1 day. Upon completion, the reaction mixture was cooled to room temperature and poured into water (100 mL); the resulting precipitate was collected at the pump, washed with water, dried, and then purified by flash column chromatography (on silica gel using dichloromethane as eluant). Recrystallization from ethanol gave the title compound **6b** as a white solid (1.39 g, 83.4%). Elemental analysis: C, 71.9; H, 8.95. $C_{50}H_{72}O_{10}$ requires: C, 71.91; H, 8.93. Mass spectrum: m/z (EI), 832 (100%). ^{1}H NMR: δ_H (CDC1$_3$) 0.93 (12H, t, J = 6.8 Hz, $Ar-O(CH_2)_5CH_3$), 1.29−1.70 (30H, m, $Ar-OCH_2CH_2(CH_2)_3$ and $Ar-OCH_2COOCH_2CH_3$), 1.94 (8H, m, $Ar-OCH_2CH_2$), 4.19−4.35 (12H, m, $Ar-OCH_2$ and $Ar-OCH_2COOCH_2$), 4.87 (4H, s, $Ar-OCH_2COO$), 7.79 (2H, s, Ar*H*), 7.82 (2H, s, Ar*H*), 7.95 (2H, s, Ar*H*).

MC BP2000 (**10**). A mixture of 2,7-dihydroxy-3,6,10,11-tetrahexyloxytriphenylene (**6a**) (5.28 g, 8 mmol), 1,12-dibromododecane (2.36 g, 7.2 mmol), and cesium carbonate (5.2 g, 16 mmol) in *N*-methyl-2-pyrrolidinone (50 mL) was heated at 110 °C for 2 days. To ensure that all of the oligomer **7** was terminated with a phenol hydroxyl group, excess of compound **6a** (0.5 g) was added, and the polymerization was continued for one more day (Figure 3i).

Ethyl 2-bromoacetate (1 g, excess) was then added to the reaction mixture. After 1 day at 110 °C, the reaction mixture was cooled and poured into water (300 mL). The resulting precipitate was collected at the pump, washed with water, and dried to yield the ester-capped oligomer **8** (Figure 3ii).

The crude ester-capped oligomer **8** and sodium hydroxide (1 g) in ethanol/water were heated under reflux for 2 days. After cooling to room temperature the reaction mixture was poured into water (200 mL), acidified with dilute hydrochloric acid, and then extracted with dichloromethane. The organic layer was washed with water and concentrated in vacuo, and then a large volume of methanol was added to precipitate the acid-capped oligomer **9** (Figure 3iii, 6.0 g, 90%).

A mixture of the acid-capped oligomer **9** (5.8 g), poly(ethylene glycol) methyl ether ($M_w \sim 2000$, 6 g), 1,3-dicyclohexyl carbodiimide (DCC, 2 g), and 4-(dimethylamino)pyridine (DMAP, 0.5 g) in dry, distilled dichloromethane (100 mL) was stirred at room temperature for 1 week. The reaction mixture was then poured into water (300 mL) and separated. The organic layer was washed with water several times, until the aqueous phase remained clean, and then concentrated in vacuo to leave a light brown amorphous solid. The crude product was purified by column chromatography (silica gel using dichloromethane, 2% methanol/dichloromethane to 5% methanol/dichloromethane as eluants), giving unreacted oligomer (1.5 g), diblock copolymer (1.9 g, 22%), and triblock copolymer **10** (Figure 3iv, 1.9 g, 22%).

^{1}H NMR: δ_H (CDC1$_3$) 0.93 (t, J = 6.8 Hz, $Ar-O(CH_2)_5CH_3$), 1.10−1.70 (m, $Ar-OCH_2CH_2(CH_2)_3$), 1.93 (m, $Ar-OCH_2CH_2$), 3.38 (s, OCH_3), 3.55−3.75 (m, centered at 3.65, OCH_2), 3.82 (m, OCH_2), 4.00 (m, OCH_2), 4.23 (t, J = 6.5 Hz, $Ar-OCH_2$), 4.40 (m, OCH_2), 4.87 (s, $Ar-OCH_2$), 7.83 (s, Ar*H*), 7.89 (s, Ar*H*). The ^{1}H NMR spectrum clearly shows peaks at 4.00 ppm, 4.40 ppm corresponding to the protons on the linker between the blocks, and the ratio of the areas of the peaks at 3.65 ppm to those peaks at 7.83 and 4.23 ppm are as expected for the triblock copolymer.

Characterization. ^{1}H NMR spectra were recorded on Bruker GE QE 300 instrument using dry $CDCl_3$ as solvent and TMS (0.03% v/v) as internal reference (0.00 ppm).

GPC were performed by EPSRC Services (RAPRA, PLgel 2x mixed bed-B, 30 cm, 10 μm), chloroform was used as an

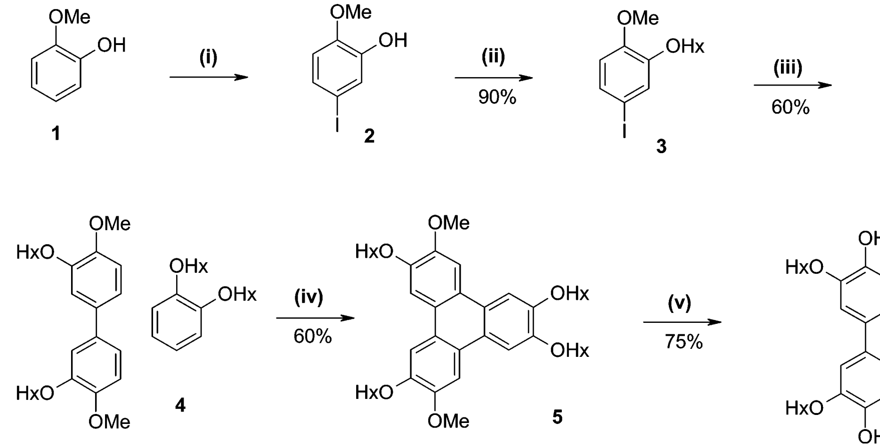

Figure 2. Synthesis of the bifunctional triphenylene monomer **6**: (i) 1. AcCl, DCM, 2. I_2, HIO_3, AcOH, DCM, H_2O, 3. K_2CO_3, MeOH, H_2O. (ii) $C_6H_{13}Br$, K_2CO_3, EtOH. (iii) Cu, heat. (iv) 1. $FeCl_3$, DCM, 2. MeOH. (v) Li, Ph_3P, THF.

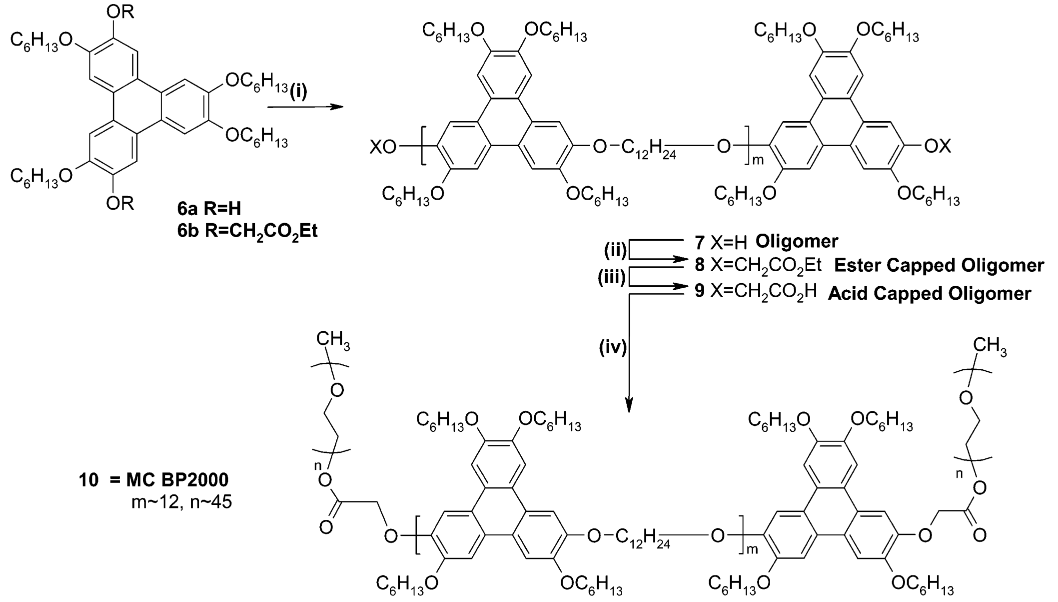

Figure 3. Synthesis of the triblock copolymer MC BP2000 **10**: (i) $Br-C_{12}H_{24}-Br$, Cs_2CO_3, NMP. (ii) $BrCH_2COOCH_2CH_3$. (iii) 1. NaOH, CH_3CH_2OH, H_2O, 2. 1 M HCl. (iv) $CH_3(OCH_2CH_2)_nOH$, DCC, DMAP, THF.

eluent at a flow rate of 1 mL min^{-1}, and molecular weights were calculated relative to polystyrene standards.

Phase behavior was studied using an Olympus BH-2 optical polarizing microscope with a Linkam hot stage and temperature controller (±0.1 K) and a Perkin-Elmer DSC7 thermal analysis system (cooling and heating rate, 10 °C/min, −40 to 200 °C).

WAXS experiments were performed using a pinhole camera consisting of a Phillips generator and tubes, nickel-filtered Cu Kα, radiation $\lambda = 0.154$ nm, and thin-walled Lindemann capillary tubes (0.5−1 mm diameter). Small-angle X-ray scattering experiments were conducted at the Synchrotron Radiation Source (SRS), Daresbury Laboratory, UK, on beamlines 8.2 and 16.1. On both stations a 3m camera was used, with wavelength $\lambda = 1.5$ Å. For SAXS/WAXS on unsheared polymer, station 8.2 was used. The sample was mounted in a DSC pan, modified with mica windows to allow transmission of the X-ray beam, and placed in a single pan Linkam DSC stage. Details of this instrument are provided elsewhere.[33] On both stations, the data were corrected for detector nonlinearity, and the q scale ($q = 4\pi \sin\theta/\lambda$ where 2θ is the scattering angle) was obtained using a specimen of wet collagen (rat tail tendon) for calibration.

Simultaneous rheology and small-angle X-ray scattering experiments were performed on beamline 16.1 using a SAXS rheometer described elsewhere.[34] The sample is mounted in a shear sandwich assembly with plates modified with apertures to allow transmission of the X-ray beam. With the rheometer in situ at the X-ray beamline, the shear direction v was vertical, and the X-ray beam was incident along the horizontal shear gradient direction ∇v, the neutral direction $\mathbf{e} = \nabla v \times v$ also being horizontal. The acquisition of SAXS and rheology was synchronized using an electronic trigger. Measurements of the dynamic shear moduli were performed using a Rheometrics solid analyzer RSA II strain-controlled system, with samples mounted in a shear sandwich configuration. The rheometer generates an oscillatory (sinusoidal) strain, and the storage and loss shear moduli, G' and G'', respectively, are measured as a function of the deformation conditions. Films for rheology experiments were prepared by dissolving the polymer in chloroform in PTFE molds. Removal of the solvent was initially conducted at room temperature in a fume cupboard. Complete removal of the solvent was later ensured by leaving the molds in a vacuum oven at 90 °C for 2 days. Order−disorder phase transition temperatures were determined from isochronal temperature ramps, performed in the linear viscoelastic regime, at the rate of 1 °C min^{-1}. Because of the very high modulus of the sample (hard solid state) at temperatures lower than 70 °C, reliable measurements could not be made on heating. However, reliable data were obtained during cooling ramps, starting from the molten state at 130 °C.

The samples for freeze-fracture TEM were heated to 85 °C (isotropic phase), slowly cooled to 40 °C, and then quenched

Table 1. GPC Data (M_w, M_n, and M_w/M_n) for the Polymers Used in This Investigation (As Compared to Polystyrene Standards)

compound	M_w	M_n	M_w/M_n
oligomer **7**[a]	28 100	7020	4.0
acid-capped oligomer **9**	12 300	4020	3.1
MC BP2000 **10** batch 1	18700	11300	1.7
MC BP2000 **10** batch 2	18500	11300	1.6

[a] Used for the extrusion of the aligned fiber which was examined by X-ray diffraction for Figure 5. A separate batch was made at a later date for conversion into the acid-capped oligomer **9**, which was used in the manufacture of MC BP2000 **10**.

with liquid nitrogen. The specimens were freeze-fractured in vacuo (3×10^{-7} Torr) at −150 °C using a Cressington CFE-50 freeze-fracture unit, coated with 1.8 nm of platinum at a 45° angle and finally with 12 nm of carbon at a 90° angle. The replicas were cleaned with chloroform, collected onto copper grids, and examined using a JEOL 1200 EX transmission electron microscope operated at 80 kV.

Results and Discussion

Synthesis. The discotic monomer 2,7-dihydroxy-3,6,10,11-tetrahexyloxytriphenylene (**6a**) was prepared as shown in Figure 2.[24] In a previous paper we described a similar polymer to MC BP2000 **10**, in which the PEO and discotic liquid crystal blocks were joined through an ether linkage.[22,23] We found that this polymer rapidly darkened on storage, a phenomenon which we attributed to the presence of diblock impurities with a free (oxygen sensitive) phenolic hydroxy group. The advantage of MC BP2000 **10** is that all of the phenolic hydroxyl groups are capped with $-CH_2CO_2H$ moieties. Hence, even if traces of diblock impurity remain, they do not easily air oxidize. Indeed, these new polymers did not significantly darken on storage.

The model ester-capped monomer 2,7-bis(2-ethoxyacetoxy)-3,6,10,11-tetrahexyloxytriphenylene (**6b**) (Figure 3) was found to exhibit the typical columnar phase sequence (Cr 88.5 °C Col$_h$ 129.2 °C I).

The hydroxyl-terminated triphenylene oligomer **7** was prepared by reacting 1,12-dibromododecane with 10% excess of the discotic monomer **6a** (Figure 3). Oligomer **7** was then “capped” with ethyl 2-bromoacetate to yield oligomer **8** (Figure 3). The ester-capped oligomer **8** was saponified to reveal the carboxylic acid functionality (**9**), which was reacted with a large excess of methoxy poly(ethylene oxide) with DCC/DAMP to give diblock and triblock copolymers **10**. The main chain triblock copolymer MC BP2000 **10** was obtained after careful repeated flash column chromatography. Attempts to produce pure, well-defined block copolymers with longer poly(ethylene oxide) blocks (e.g., MC BP5000) failed, as it proved impossible to remove excess PEO5000 at the end of the reaction. In the case of shorter PEO blocks (for example, MC BP750), the phase behavior was unremarkable, and our efforts to characterize the block copolymers have therefore concentrated on the single block copolymer MC BP2000 **10**.

Size-Exclusion Gel Permeation Chromatography. The average molecular weights and polydispersity for the triblock copolymers as determined by GPC are shown in Table 1. MC BP2000 **10** has a weight-average molecular weight (M_w) of ~18 600, with a polydispersity (M_w/M_n) of ~1.65 (across two different batches). Based on the measured masses and densities of the discotic liquid crystal and poly(ethylene oxide) regions, the volume fraction poly(ethylene oxide) in BP2000 **10** (ϕ_{PEO}) is ~27%.

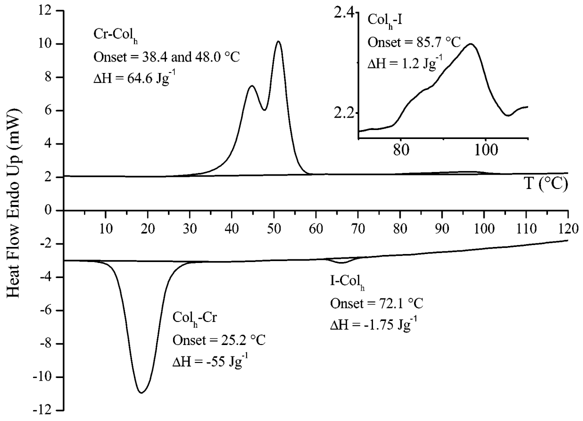

Figure 4. DSC thermogram showing heat flow (mW) vs temperature (°C) for MC BP2000 **10b** (batch 2, upper = heating, lower = cooling). The phase assignment, onset temperatures, and enthalpy changes for each transition are given; the inset (top right) shows a close-up of the peak measured at the Col$_h$−I transition on the first heating run.

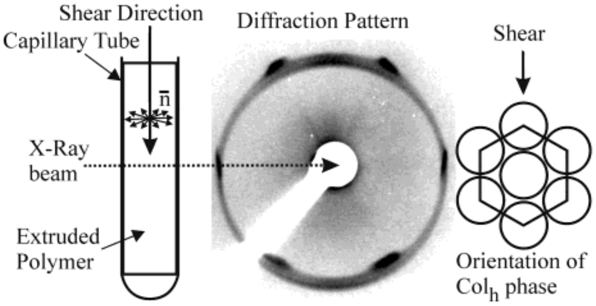

Figure 5. Diffraction pattern of an extruded fiber of the main chain triphenylene oligomer **7** (extruded through a pinhole die (1 mm diameter) with a barrel temperature of 100 °C and a die temperature of 90 °C). The diffraction pattern shows hexagonal symmetry, which is consistent with the columnar arrangement shown.

Thermal Analysis. DSC (Table 2) shows phase transitions for the triblock copolymer **10** and its components. Upon heating, there is a broad endothermic transition corresponding to the clearing point of the crystalline PEO block, followed, at higher temperatures, by a smaller transition corresponding to the clearing point of the triphenylene block (Figure 4). The temperatures and enthalpies of these transitions are summarized in Table 2. Upon cooling the same phase sequence is observed, though the transition temperatures are somewhat lower due to supercooling. Upon second and subsequent heating and cooling runs the DSC trace remains essentially unaltered.

X-ray Diffraction Experiments. A separately prepared sample of oligomer **7** (M_w = 24 000) shows a Col$_h$ mesophase between 98 and 118 °C. At 112 °C the X-ray diffraction peaks show an intracolumnar distance of 3.5 Å and an intercolumnar distance of 17.3 Å with the two inner rings of the diffraction pattern showing the $1:\sqrt{3}$ relationship characteristic of reflections from a hexagonal lattice.[24] Under shear (for example, when the polymer is extruded as a fiber; Figure 5) the columns are oriented perpendicular to the shear direction, consistent with the polymer backbone being extended along the direction of shear. Hence, for an extruded fiber the inner 17.5 Å reflection of the diffraction pattern no longer appears as a ring but clearly shows hexagonal symmetry (Figure 5).

Table 2. Thermal Behavior of the Relevant Compounds As Determined by DSC and Optical Polarizing Microscopy[a]

compound	first heating	first cooling	second heating
model compound **6b**	Cr 88.5 Col_h 129.2 I		
oligomer **9**	Col_h 106 (3.13) I	I 90.1 (−3.83) Col_h	Col_h 104.7 (3.02)
PEO2000	Cr 53.8 (182.7) I	I 40.6 (−159.9) Cr	Cr 51.5 (164.7) I
9 + PEO2000 1:2	Cr 49.2 (44.9) Col_h 113.2 (2.5) I	I 94.2 (−2.8) Col_h 40.0 (−39.5)* Cr	Cr 50.8 (43.6) Col_h109.2 (2.17) I
MC BP2000 **10** batch 1	Cr 39.2/48.6 (61.6) Col_h 84.1 (1.4) I	I 70.9 (−1.5) Col_h 25.3 (−55.2) Cr	Cr 41/48.6 (56.8) Col_h 86.3 (1.3) I
MC BP2000 **10** batch 2	Cr 38.4/48.0 (64.6) Col_h 85.7 (1.2) I	I 72.1 (−1.75) Col_h 25.2 (−55) I	Cr 40.5/48.6 (55.6) Col_h 89.2 (0.91) I

[a] Phase transition temperatures are indicated in °C and transition enthalpies in J g^{-1} (bracketed).

Table 3. Summary of Wide-Angle X-ray Diffraction Data for MC BP2000 10

temperature	distance	comment
RT, 40 °C	5.1, 4.1 Å	typical crystalline PEO diffraction
	19 Å	intercolumnar (column−column) separation
60 °C, 75 °C	sharp 3.9 Å	intracolumnar (core−core) separation
	diffuse halo ~4.5 Å	alkyl side chain
	sharp 19 Å	intercolumnar (column−column) separation
110 °C, 125 °C	no peak at 3.9 Å	intracolumnar (core−core) separation
	very weak halo ~4.5 Å	alkyl side chain
	very weak 19 Å	intercolumnar (column−column) separation

The hexagonal nature of the columnar phase exhibited by the triphenylene-containing phase-separated regions in the block copolymer MC BP2000 **10** was confirmed using wide-angle X-ray diffraction (WAXS; Table 3). For the microphase-separated material at room temperature and 40 °C the diffraction pattern consists of sharp rings corresponding to crystalline PEO regions and a hexagonal repeat of 19 Å corresponding to the column−column separation of the discotic liquid crystal. The reflections at 3.9 and 4.5 Å also expected for the columnar phase are masked by the strong reflections from crystalline poly(ethylene oxide). As the temperature is increased to 60 °C, the poly(ethylene oxide) regions melt, revealing a diffraction pattern typical of the columnar hexagonal mesophase. At temperatures above the clearing point (>85 °C) the columnar ordering is lost, and the diffraction pattern is comprised of broad peaks corresponding to the scattering from a disordered melt.

The microphase-separated structure of MC BP2000 **10** was further characterized by small-angle X-ray scattering (SAXS) over the temperature range 30−200 °C (Figure 6). Selected scans are shown in Figure 7. At T = 30 °C, SAXS indicates a lamellar microphase-separated structure, with peaks in the positional ratio 1:2. At these temperatures the PEO-containing regions are crystalline.

Melting of the PEO regions was associated with a discontinuous change in the SAXS profile (position and intensity of reflections) at $T = 45 \pm 3$ °C, in good agreement with the DSC data. At $T = 70$ °C (Figures 5 and 6) the peak at $q^* = 0.037 \pm 0.001$ Å^{-1} corresponds to a microphase-separated structure with a domain spacing $d = 170 \pm 5$ Å. There is evidence for a weak, higher order reflection, centered on approximately $3q^*$ (which is more clearly seen in the X-ray diffractogram of the oriented microphase-separated polymer in Figure 8). This is consistent with a hexagonal-packed columnar phase. A further discontinuous change in SAXS peak width, intensity and position occurred, starting at T = 87 °C, close to the Col_h−I transition identified by DSC and optical polarizing microscopy (OPM). The SAXS profile in Figure 7 indicates that the high-temperature phase is characterized by a single weak reflection, suggesting that this is a disordered microphase-separated structure.

Oscillatory Shear. Shear experiments were performed to assess the possibility of producing aligned samples and to clarify the nature of the phase-separated structure. Previous work carried out on extruded samples of main-chain triphenylene polymers (such as **7**) has

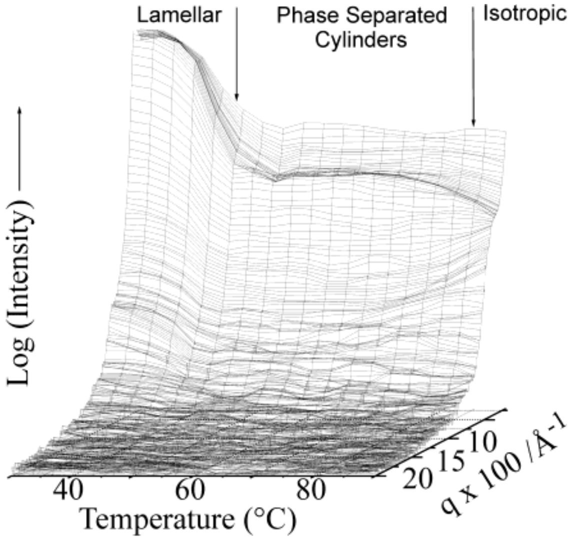

Figure 6. Temperature dependence of the small-angle X-ray diffraction as a function of the scattering vector **q**.

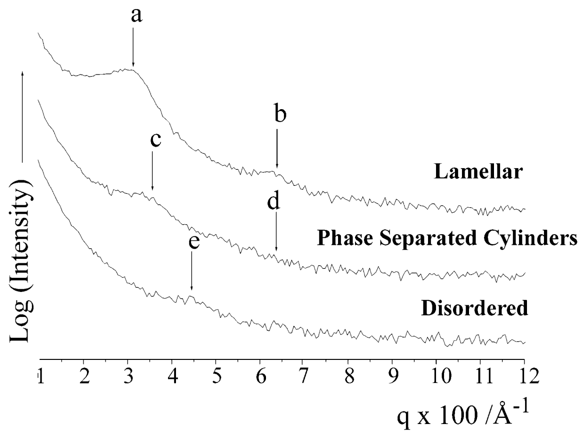

Figure 7. Sections through Figure 6 showing log(intensity) vs **q** at different temperatures. The important peaks are highlighted. a: $q = 3.2 \times 10^{-2}$ Å^{-1}, d = 196 Å. b: $q = 6.4 \times 10^{-2}$ Å^{-1}, d = 98 Å. c: $q = 3.7 \times 10^{-2}$ Å^{-1}, d = 170 Å. d: $q = 6.4 \times 10^{-2}$ Å^{-1}, d = 98 Å. e: $q = 4.4 \times 10^{-2}$ Å^{-1}, d = 143 Å.

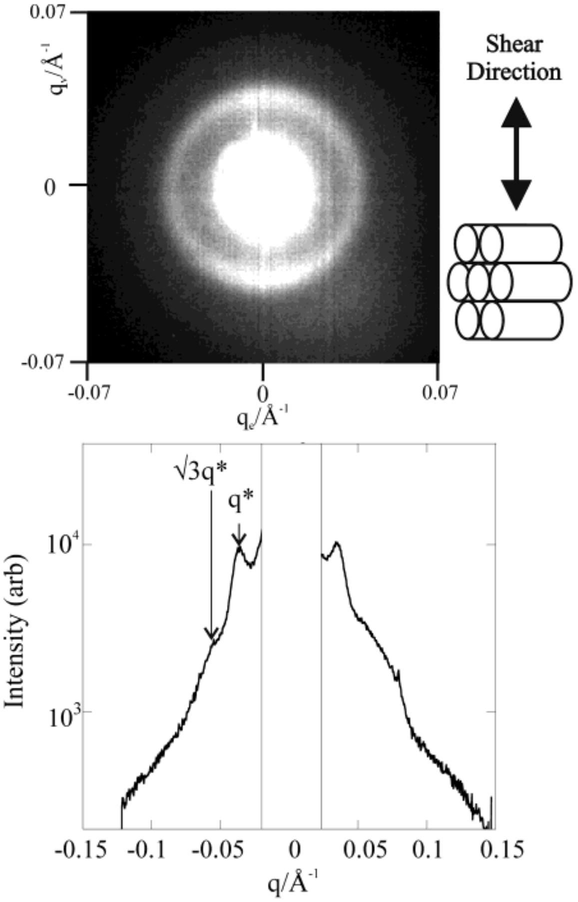

Figure 8. Small-angle X-ray diffraction pattern for the microphase-separated hexagonal columnar phase of MC BP2000 **10** under dynamic shear ($w = 10$°/s, $\gamma = 400\%$) at 70 °C. Top: the full diffraction pattern indicative of an aligned columnar phase with the columns laying perpendicular to the shear direction (as indicated top right). Bottom: a vertical slice of the SAXS pattern in which a 1:3 repeat clearly shows the presence of a hexagonal phase.

shown that the polymer chains align preferentially along the direction of shear (Figure 5), thus forcing the columns of the hexagonal columnar discotic liquid crystal to lie perpendicular to the direction of shear. In MC BP2000 **10** simultaneous X-ray diffraction measurements on samples subjected to large-amplitude oscillatory shear show that the columns of PEO lie perpendicular to the shear direction (Figure 8); i.e., they lie parallel to the $\mathrm{Col_h}$ director (n) and perpendicular to the extended polymer chain. There is a strong interplay between the alignment of the $\mathrm{Col_h}$ triphenylene regions and that of the bulk, microphase-separated polymer (Figure 8) since, in most copolymer systems exhibiting a columnar phase, the microphase-separated cylindrical structures are normally aligned parallel to the shear direction.[32] The unexpected parallel arrangement of the phase-separated cylinders is further evidence that there are a number of factors that may be important in determining the relationships between block copolymer morphology and liquid crystalline order. *In the case of this particular triphenylene block copolymer the orientation of both columnar and cylindrical phases is driven by the stretching of the polymer chains along the direction of shear (Figure 12).*

Figure 9 shows the measured loss and storage moduli as a function of temperature for MC BP2000 **10**. Upon cooling from the melt, a sharp increase in the viscosity was observed at $T \sim 95$ °C, consistent with the I−$\mathrm{Col_h}$ transition observed by DSC. At lower temperatures the viscosity of the sample increases further, breaching the operational limits of the apparatus at <70 °C.

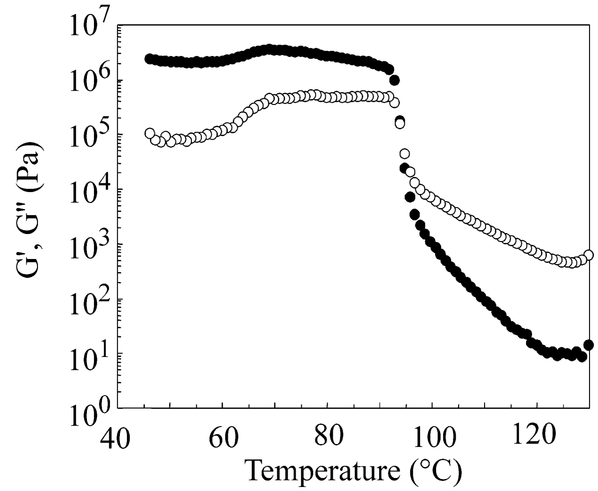

Figure 9. Temperature dependence of logarithmic storage modulus G' (●) and loss modulus G'' (○) for a film of MCBP2000 **10** during a cooling ramp (1 °C min^{-1}, $w = 10$ rad s^{-1}, $\gamma = 1\%$). The arrow indicates the transition temperature $T = 93$ °C. The distortions below 68 °C are due to the increasing viscosity of the sample, close to the limits of the rheometer. Below 46 °C these limits were reached and the apparatus overloaded.

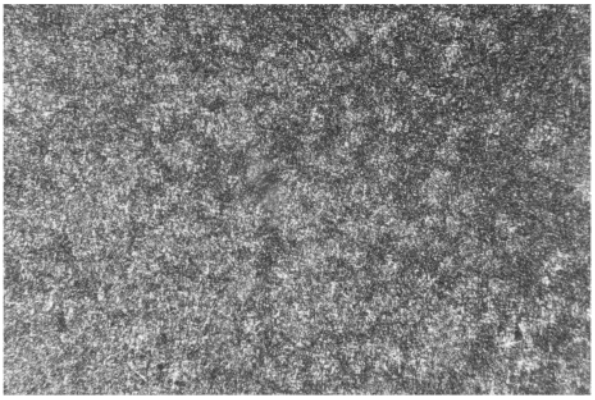

Figure 10. Texture of the $\mathrm{Col_h}$ phase of MCBP2000 **10** as it appears when viewed through crossed polarizing filters (×200) at 80 °C. The sample was slowly cooled from the melt at 0.1 °C min^{-1} and annealed at 80 °C for 3 days.

Microscopy. Polarizing optical microscopy shows that, below the $\mathrm{Col_h}$−I transition, MC BP2000 **10** has a sandy or threaded texture (Figure 10), a feature found in many sorts of polymeric triphenylene-based discotic liquid crystals, but not of use in identifying the phase.[22,23] No long-range alignment or microphase separation is observed even after annealing for several days.

Electron Microscopy. Freeze-fracture electron microscopy (Figure 11) confirms the lamellar arrangement at 40 °C and shows the presence of lamellae extending over 0.2 μm. Their spacing $d \sim 170$ Å (measured directly from the photomicrographs) is comparable to that determined by SAXS. These images are very similar to those of other block copolymers.[35−38]

Discussion and Conclusion

If amphiphiles are created that embody the molecular architecture of a discogen (rather than the hydrophilic “head”/hydrophobic “tail” molecular architecture of a

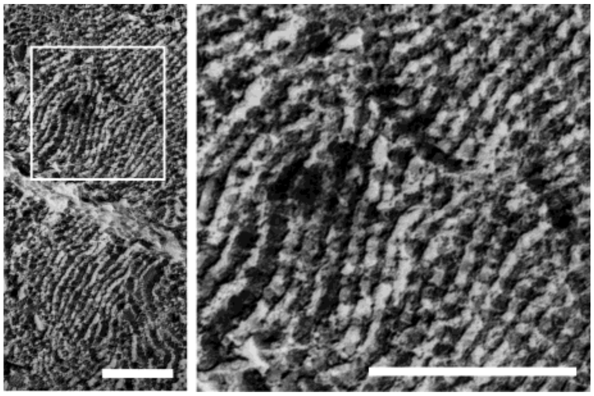

Figure 11. Electron micrograph of a freeze-fractured sample of MC BP2000 **10** (scale bar = 200 nm). The sample was quenched from 40 °C (in the lamellar phase). The section of the micrograph marked with a box is enlarged on the right-hand side, clearly showing the lamellar structure.

conventional soap), columnar and nematic (N_C) liquid crystal phases are found to totally dominate the phase diagram[39−42] and cubic and lamellar phases are eliminated. Hence, the phase behavior for the water/amphiphile system is greatly simplified. An additional technological advantage is also created because it becomes easy to prepare bulk-aligned samples using surface forces and magnetic fields. Similar advantages accrue for block copolymers in which one component is a discotic liquid crystal.[43] Depending on temperature and volume fraction, most block copolymers give a range of lamellar, columnar, or cubic microphase-separated structures.[4,32] However, if there is an underlying columnar discotic architecture, it should be easy for these copolymers to form columnar microphase-separated structures whereas cubic microphase-separated structures seem highly unlikely to form. As is the case with the lyotropic systems, we should obtain a simplified phase behavior (Figure 1). Furthermore, the alignment of the microphase-separated regions should reflect, and be controlled by, that of the underlying discotic columnar mesophase. In this paper we have shown that a triblock copolymers in which a main chain polymeric discotic liquid crystal is capped at both ends with blocks of PEO[23] undergoes microphase separation to give columnar (but not cubic) superstructures, and crystallization of the PEO chains leads to a lamellar phase. As expected, the alignment of these is dictated by that of the underlying mesophase. Hence, under shear, the columnar superstructures in the hexagonal phase, like the molecular columns in a main chain discotic polymer, orient perpendicular to the shear direction.[24−31] This contrasts with the hexagonal phases of most phase-separated block copolymers where the columns orient parallel to the shear direction. Hexagonally packed PEO cylinders with a periodicity of 170 Å form in a continuous discotic liquid crystal matrix as indicated by the SAXS pattern (Figure 7). If a completely aligned hexagonal arrangement of cylinders and discotic cores is assumed, then the diameters of the cylinders and their interstitial distance can be estimated. This calculation predicts that the cylinders will have a radius of about 70 Å with a spacing of 240 Å between them (in the

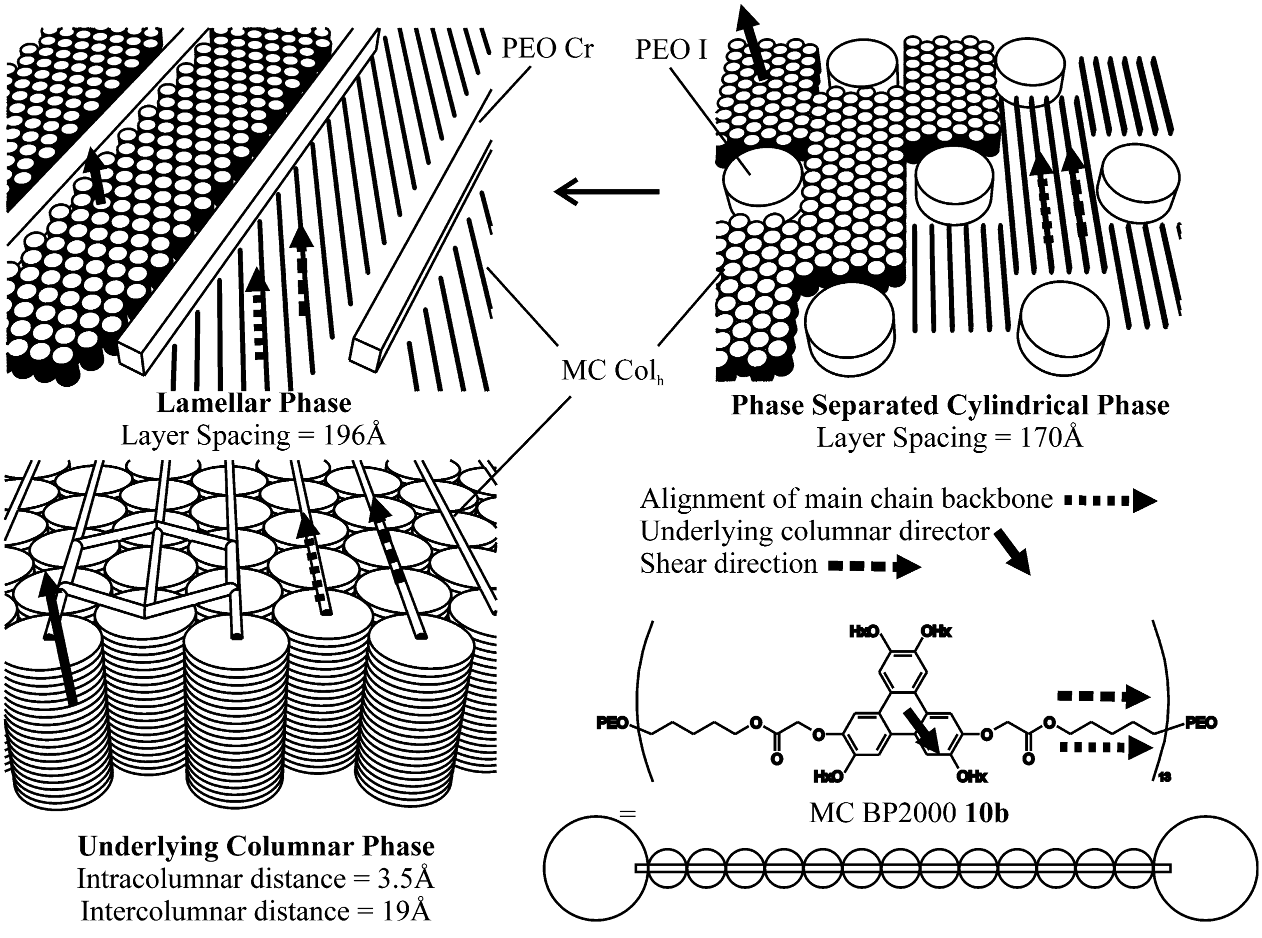

Figure 12. Summary of the relationships between the orientations of the microphase-separated structures with those of the underlying discotic liquid crystal in MCBP2000 **10**.

arrangement shown in Figure 12). This is enough space for 13 discotic main chain units, which agrees well with the GPC data. An additional subtlety shown in Figure 12b,c is that in the columnar microphase-separated superstructure the polymer chains bridge from one poly(ethylene oxide) “rod” to its *next*-nearest neighbor. In other words, the columnar hexagonal superstructure is oriented “apex-on” rather than “edge-on” relative to the shear direction. It is easy to show, using a simple space-filling model (the elements in Figure 12 are roughly to scale), that an arrangement in which the polymer chains bridge from one poly(ethylene oxide) “rod” to its *nearest* neighbor and in which the hexagonal superstructure is oriented “apex-on” to the direction of shear is not possible for **10** but that it should be possible to switch from “side-on” to “edge-on” by changing the relative volume fractions of the blocks. When the poly(ethylene oxide) chains crystallize and the lamellae form, these should be formed at ±60° to the original shear direction as shown in Figure 12a. Further attempts to explore the phase behavior and alignment properties of these and other block copolymers in which one component has the underlying substructure of a discotic liquid crystal are in progress.

Acknowledgment. The authors thank the EPSRC and NEDO for financial support, Paul Unwin for use of wide-angle X-ray apparatus, and EPSRC GPC Services (RAPRA technology) for molecular weight measurements.

References and Notes

(1) McCardle, C. B., Ed. *Side Chain Liquid Crystal Polymers*; Blackie: London, 1989.
(2) Hsu, C.-S. *Prog. Polym. Sci.* **1997**, *22*, 829−871.
(3) Yoshimoto, N.; Hanna, J. *Adv. Mater.* **2002**, *14*, 988.
(4) Hamley, I. W. *The Physics of Block Copolymers*; Oxford University Press: Oxford, 1998.
(5) Poser, S.; Fischer, H.; Arnold, M. *Prog. Polym.* **1998**, *23*, 1337−1379.
(6) Anthamatten, M.; Zhang, W. Y.; Hammond, P. T. *Macromolecules* **1999**, *32*, 4838−4848.
(7) Fischer, H.; Poser, S.; Arnold, M. *Liq. Cryst.* **1995**, *18*, 503−509.
(8) Anthamatten, M.; Wu, J.-S.; Hammond, P. T. *Macromolecules* **2001**, *34*, 8574−8579.
(9) Walther, M.; Finkelmann, H. *Prog. Polym. Sci.* **1996**, *21*, 951−979.
(10) Hamley, I. W. *Adv. Polym. Sci.* **1999**, *148*, 113−137.
(11) Fischer, H.; Poser, S.; Arnold, M.; Frank, W. *Macromolecules* **1994**, *27*, 7133−7138.
(12) Mao, G.; Wang, J.; Clingman, S. R.; Ober, C. K.; Chen, J. T.; Thomas, E. L. *Macromolecules* **1997**, *30*, 2556−2567.
(13) Adams, J.; Gronski, W. In *Liquid Crystal Polymers*; Ober, C. K., Ed.; American Chemical Society: Washington, DC, 1990; Vol. 433.
(14) Yamada, M.; Iguchi, T.; Hirao, A.; Nakahama, S.; Watanabe, J. *Macromolecules* **1995**, *28*, 50−58.
(15) Zheng, W.-Y.; Albalak, R. J.; Hammond, P. T. *Macromolecules* **1998**, *31*, 2686−2689.
(16) Anthamatten, M.; Hammond, P. T. *Macromolecules* **1999**, *32*, 8066−8076.
(17) Zheng, W. Y.; Hammond, P. T. *Macromolecules* **1998**, *31*, 711−721.
(18) Sänger, J.; Gronski, W.; Maas, S.; Stühn, V.; Heck, B. *Macromolecules* **1997**, *30*, 6783−6787.
(19) Zheng, W. Y.; Hammond, P. T. *Macromolecules* **1998**, *31*, 711−721.
(20) Zheng, W. Y.; Albalak, R. J.; Hammond, P. T. *Macromolecules* **1998**, *31*, 2686−2689.
(21) Anthamatten, M.; Zheng, W. Y.; Hammond, P. T. *Macromolecules* **1999**, *32*, 4838−4848.
(22) Boden, N.; Bushby, R. J.; Lu, Z. B.; Eichhorn, H. *Mol. Cryst. Liq. Cryst. Sci. Technol., Sect. A: Mol. Cryst. Liq. Cryst.* **1999**, *332*, 2791−2801.
(23) Boden, N.; Bushby, R. J.; Eichhorn, H.; Lu, Z. B.; Abeysekera, R.; Robardes, A. W. *Mol. Cryst. Liq. Cryst. Sci. Technol., Sect. A: Mol. Cryst. Liq. Cryst.* **1999**, *332*, 2803−2812.
(24) Boden, N.; Bushby, R. J.; Cammidge, A. N. *J. Am. Chem. Soc.* **1995**, *117*, 924−927.
(25) Boden, N.; Bushby, R. J.; Cammidge, A. N. *J. Chem. Soc., Chem. Commun.* **1994**, 465−466.
(26) Boden, N.; Bushby, R. J.; Cammidge, A. N.; Martin, P. S. *J. Mater. Chem.* **1995**, *5*, 1857−1860.
(27) Kreuder, W.; Ringsdorf, H.; Tschirner, P. *Makromol. Chem., Rapid Commun.* **1985**, *6*, 367−373.
(28) Ringsdorf, H.; Tschirner, P.; Hermannschonherr, O.; Wendorff, J. H. *Makromol. Chem., Macromol. Chem. Phys.* **1987**, *188*, 1431−1445.
(29) Stewart, D.; McHattie, G. S.; Imrie, C. T. *J. Mater. Chem* **1998**, *8*, 47−51.
(30) Talroze, R. V.; Otmakhova, O. A.; Koval, M. A.; Kuptsov, S. A.; Plate, N. A.; Finkelmann, H. *Macromol. Chem. Phys.* **2000**, *201*, 877−881.
(31) Werth, M.; Spiess, H. W. *Makromol. Chem., Rapid Commun.* **1993**, *14*, 329−338.
(32) Hamley, I. W. *J. Phys.: Condens. Matter* **2001**, *13*, R643−R671.
(33) Bras, W.; Derbyshire, G. E.; Devine, A.; Clark, S. M.; Cooke, J.; Komanschek, B. E.; Ryan, A. J. *J. Appl. Crystallogr.* **1995**, *28*, 26−32.
(34) Hamley, I. W.; Pople, J. A.; Gleeson, A. J.; Komanschek, B. U.; Towns-Andrews, E. *J. Appl. Crystallogr.* **1998**, *31*, 881−889.
(35) Molenberg, A.; Sheiko, S.; Moller, M. *Macromolecules* **1996**, *29*, 3397−3400.
(36) Eisenbach, C. D.; Goldel, A.; Terskan-Reinold, M.; Schubert, U. S. *Colloid Polym. Sci.* **1998**, *276*, 780−785.
(37) Zheng, R. Q.; Chen, E. Q.; Cheng, S. Z. D.; Xie, F. C.; Yan, D. H.; He, T. B.; Percec, V.; Chu, P. W.; Ungar, G. *Macromolecules* **1999**, *32*, 6981−6988.
(38) Zheng, R. Q.; Chen, E. Q.; Cheng, S. Z. D.; Xie, F. C.; Yan, D. H.; He, T. B.; Percec, V.; Chu, P. W.; Ungar, G. *Macromolecules* **2000**, *33*, 5159−5168.
(39) Boden, N.; Bushby, R. J.; Hardy, C. *J. Phys., Lett.* **1985**, *46*, L325−L328.
(40) Boden, N.; Bushby, R. J.; Ferris, L.; Hardy, C.; Sixl, F. *Liq. Cryst.* **1986**, *1*, 109−125.
(41) Boden, N.; Bushby, R. J.; Hardy, C.; Sixl, F. *Chem. Phys. Lett.* **1986**, *123*, 359−364.
(42) Hughes, R.; Smith, A.; Bushby, R.; Movaghar, B.; Boden, N. *Mol. Cryst. Liq. Cryst. Sci. Technol., Sect. A: Mol. Cryst. Liq. Cryst.* **1999**, *332*, 3057−3067.
(43) Cammidge, A. N.; Bushby, R. J. In *Handbook of Liquid Crystals*; Schmidt, H. J., Ed.; VCH: New York, 1997; Vol. 2.

MA020748X